Radiotherapy and Oncology 156 (2021) 80–94

Contents lists available at ScienceDirect

Radiotherapy and Oncology

journal homepage: www.thegreenjournal.com

Original Article

ESTRO ACROP guideline for target volume delineation of skull base tumors

Stephanie E. Combs [a,b,c], Brigitta G. Baumert [d], Martin Bendszus [e], Alessandro Bozzao [f], Michael Brada [g], Laura Fariselli [h], Alba Fiorentino [i], Ute Ganswindt [j], Anca L. Grosu [k,l], Frank L Lagerwaard [m], Maximilian Niyazi [c,n], Tufve Nyholm [o], Ian Paddick [p], Damien Charles Weber [q], Claus Belka [n], Giuseppe Minniti [r,s,*]

[a] *Department of Radiation Oncology, Technical University of Munich;* [b] *Institute of Radiation Medicine, Department of Radiation Sciences, Helmholtz Zentrum München;* [c] *German Cancer Consortium (DKTK) Partner Site (DKTK), Munich, Germany;* [d] *Institute of Radiation Oncology, Cantonal Hospital Graubuenden, Chur, Switzerland;* [e] *Department of Neuroradiology, University Hospital Heidelberg, Germany;* [f] *Dipartimento NESMOS, Università Sapienza Roma, Azienda Ospedaliera Sant'Andrea, Rome, Italy;* [g] *Department of Radiation Oncology, Clatterbridge Cancer Centre NHS Foundation Trust, Bebington, United Kingdom;* [h] *Radiotherapy Unit, Fondazione IRCCS Istituto Neurologico Carlo Besta, Milan;* [i] *Radiation Oncology Department, General Regional Hospital F. Miulli, Acquaviva delle fonti, Italy;* [j] *Department of Therapeutic Radiology and Oncology, Medical University of Innsbruck, Innsbruck, Austria;* [k] *Department of Radiation Oncology, Medical Faculty, University of Freiburg, Freiburg;* [l] *German Cancer Consortium (DKTK) Partner Site Freiburg, Germany;* [m] *Department of Radiation Oncology, Amsterdam University Medical Centers, Location VUmc, The Netherlands;* [n] *Department of Radiation Oncology, University Hospital, LMU Munich, Munich, Germany;* [o] *Department of Radiation Sciences, Radiation Physics, Umeå University, Umeå, Sweden;* [p] *Queen Square Radiosurgery Centre, National Hospital for Neurology and Neurosurgery, London, United Kingdom;* [q] *Centre for Proton Therapy, Paul Scherrer Institut, Villigen PSI, Switzerland;* [r] *Department of Medicine, Surgery and Neuroscience, University of Siena, Siena; and* [s] *IRCCS Neuromed, Pozzilli, Italy*

ARTICLE INFO

Article history:
Received 30 October 2020
Accepted 13 November 2020
Available online 10 December 2020

Keywords:
Skull base tumors
Target volumes
Radiotherapy
Consensus guidelines

ABSTRACT

Background and purpose: For skull base tumors, target definition is the key to safe high-dose treatments because surrounding normal tissues are very sensitive to radiation. In the present work we established a joint ESTRO ACROP guideline for the target volume definition of skull base tumors.

Material and methods: A comprehensive literature search was conducted in PubMed using various combinations of the following medical subjects headings (MeSH) and free-text words: "radiation therapy" or "stereotactic radiosurgery" or "proton therapy" or "particle beam therapy" and "skull base neoplasms" "pituitary neoplasms", "meningioma", "craniopharyngioma", "chordoma", "chondrosarcoma", "acoustic neuroma/vestibular schwannoma", "organs at risk", "gross tumor volume", "clinical tumor volume", "planning tumor volume", "target volume", "target delineation", "dose constraints". The ACROP committee identified sixteen European experts in close interaction with the ESTRO clinical committee who analyzed and discussed the body of evidence concerning target delineation.

Results: All experts agree that magnetic resonance (MR) images with high three-dimensional spatial accuracy and tissue-contrast definition, both T2-weighted and volumetric T1-weighted sequences, are required to improve target delineation. In detail, several key issues were identified and discussed: i) radiation techniques and immobilization, ii) imaging techniques and target delineation, and iii) technical aspects of radiation treatments including planning techniques and dose-fractionation schedules. Specific target delineation issues with regard to different skull base tumors, including pituitary adenomas, meningiomas, craniopharyngiomas, acoustic neuromas, chordomas and chondrosarcomas are presented.

Conclusions: This ESTRO ACROP guideline achieved detailed recommendations on target volume definition for skull base tumors, as well as comprehensive advice about imaging modalities and radiation techniques.

The skull base is an anatomically complex area encompassing portions of the anterior cranial fossa, clivus, petrous bone, middle cranial fossa, cavernous sinus and infratemporal fossa that includes critical endocrine, nervous, and vascular structures. Skull base tumors represent a very heterogeneous group of lesions with different degrees of aggressiveness; most common histologic types

* Corresponding author at: Department of Medicine, Surgery and Neuroscience, University of Siena, Siena, Italy.
E-mail address: giuseppe.minniti@unisi.it (G. Minniti).

https://doi.org/10.1016/j.radonc.2020.11.014
0167-8140/

include meningioma, pituitary adenoma, acoustic neuroma, craniopharyngioma, chordoma and chondrosarcoma.

Due to the intricate anatomy of the skull base, any treatment can potentially be associated with severe side effects; therefore, interdisciplinary decision making is essential. Only recently, several clinical practice guidelines have provided recommendations for the management of skull base tumors [1–6]. In most cases, surgery is the first step in treating skull base tumors and the vast majority of patients can be successfully treated by surgical resection alone, notably those with less aggressive and favorably located tumors. Radiation therapy (RT) is usually recommended to improve local tumor control in patients with incomplete resection of large tumors at higher risk of surgical complications and in those with completely resected tumors that display histological features associated with aggressive behavior [7–13]. In addition, RT has been established as an effective first-line treatment for selected tumors, e.g. vestibular schwannoma or cavernous sinus meningioma [3,6]. Additionally, data available today for RT indications includes large and pooled series from experienced institutions underlining the growing role of RT in the interdisciplinary context [14].

The radiation oncologist is challenged in the skull base region. Over the years, technological advances have led to improvements in every step of the radiation treatment process, including imaging techniques, treatment planning, dose delivery, and accuracy of patient repositioning. Modern stereotactic treatment techniques, either stereotactic radiosurgery (SRS) or stereotactic radiotherapy (SRT), using Gamma Knife (GK), CyberKnife (CK), and dedicated linear accelerator (LINAC)-based technologies, have resulted in further improvement of target dose coverage, conformity and organs at risk (OARs) sparing. In addition, there has been a renewed interest in using particle therapy for such tumors due to technological advances in the delivery of proton and carbon ion RT [15–17]. Along with greater accuracy of dose delivery and patient repositioning, more improvements in imaging techniques such as new sequences in MRI or novel tracers for PET-imaging have enabled tumor spatial accuracy, contributing to reduce inter-observer variability in target delineation [18–20]. As for other steps in the treatment planning process, an accurate delineation of tumor volumes and OARs is mandatory for a precise calculation of the spatial dose distribution, and for choosing the optimal radiation dose and fractionation schedule.

The purpose of the present guideline article is to provide recommendations on target volume delineation for skull base tumors.

Methods and materials

An ESTRO task force of 16 European experts consisting of radiation oncologists (12), neuroradiologists (2) and physicists (2) discussed and analyzed the body of evidence concerning skull base tumors target delineation. The PubMed database was searched using combinations of the following medical subjects headings (MeSH) and free-text words: "radiation therapy" or "stereotactic radiosurgery" or "proton therapy" or "particle beam therapy" and "skull base neoplasms" "pituitary neoplasms", "meningioma", "craniopharyngioma", "chordoma", "chondrosarcoma", "acoustic neuroma/vestibular schwannoma", "organs at risk", "gross tumor volume", "clinical tumor volume", "planning tumor volume", "target volume", "target delineation", "dose constraints". In parallel, abstracts from ESTRO and ASTRO were analyzed. Searches were completed by May 15, 2020. Based on the initial searches, a total of 8483 articles and abstracts were identified. With the participation of all authors, 171 relevant papers containing data on target delineation of skull base tumors and clinical outcomes following photon or proton RT in adult patients were chosen for the final guidelines. Open questions were identified and decisions were met according to the majority view.

Results

Preparation

For treatment planning, patients are generally placed in the supine position with the head fixed using an individual mask system, commonly a thermoplastic mask. In general, a neutral position usually ensures a good position reproducibility and high treatment accuracy throughout the course of treatment; however, a flexed head position is performed in some centers since tilting can facilitate a simpler beam arrangement above the eyes.

With SRS, which traditionally refers to the use of frame-based SRS, a stereotactic head frame is typically fixed to the skull under local anesthesia. As onboard imaging has advanced, SRS technology has evolved with the development of frameless SRS, with patients who are usually immobilized in a high precision mask fixation system and the SRS dose is precisely delivered with approximately 1-mm targeting accuracy to intracranial targets in one to five fractions via stereotactic guidance [21]. Currently, there are several terms that have been used interchangeably for fractionated SRS; they include "multi-fraction SRS", "multi-dose SRS", "multi-session SRS", "hypofractionated SRS", "hypofractionated stereotactic radiotherapy". With the same fixation systems and level of accuracy, the dose can be delivered in more than five fractions, so-called stereotactic RT (SRT) using either conventionally fractionated (1.8–2.0 Gy per fraction) or hypofractionated (fraction sizes greater than 2 Gy) schedules. Several commercial stereotactic mask fixation systems are currently available with a reported repositioning accuracy of 1–3 mm [22]. A customized mouth-bite attached to a thermoplastic cast that conforms to the teeth and/or maxilla is used in some centers with similar accuracy.

A computed tomography (CT) scan should be performed using thin slice, generally 1–2 mm thickness from the vertex to the bottom of the third cervical vertebra (C3). Intravenous contrast should be considered for all patients with enhancing tumors when MRI fusion is unavailable or if additional information from a contrast-enhanced CT will be used for treatment planning.

Imaging for treatment planning

Magnetic resonance imaging (MRI) using pre- and post-contrast T1-weighted and T2-weighted images is mandatory for precise radiation treatment of skull base tumors. Improvements for treatment planning accuracy include correction of geometric distortion in MR images, minimization of the time interval between MRI and treatment delivery, and the use of specific sequences for target delineation. Several mechanisms may cause significant distortions in MR images and jeopardize precise treatment delivery [23–27]. Image distortions causing significant GTV displacement arise mainly from magnetic field inhomogeneities and gradient field nonlinearities [26,27], and typically increase with distance from the isocenter and at air-bone interfaces, e.g. tumors near the paranasal sinuses and mastoid cells [24,25]. Minimization of image distortion to less than 1 mm can be obtained by using three-dimensional (3D) vendor specific geometric distortion correction algorithms, patient-specific active shimming in the scanner software, higher readout bandwidth, and isotropic 3D sequences [28]. Performing MRI in the treatment position with an immobilization mask could reduce errors due to nonrigid tissue deformation and uncertainties related to image registration; however, similar high registration accuracy can be obtained using planning CT and MR images with a thin (1 mm) slice thickness while maintaining the head and neck in a neutral position. Registration

between MR and CT should be carefully reviewed; in presence of different head extension, registration accuracy can be increased by using the region of interest instead of the whole head.

The time interval between imaging and treatment delivery should be as short as possible; the interval should not exceed one week in patients with aggressive and malignant tumors due to the high risk of tumor increase or resection cavity volume changes, whereas longer time intervals up to three-four weeks can be safely applied in those with benign tumors.

MR images should be discussed with the radiologist, since requirements on MRI for RT may differ from routine diagnostic imaging. Contrast-enhanced 3D fast gradient echo T1-weighted sequences obtained with a voxel size of 1 × 1 × 1 mm, named MPRAGE, 3D FLASH, 3D FGRE, 3D FSPGR, 3D TFE, 3D FFE depending on the manufacturer, should be recommended for their high spatial resolution and accurate characterization of subtle enhancement patterns in the surrounding neurovascular structures, and along the course of the optic nerves [29–31]. In addition, they allow reformatting of 3D data for viewing in all three planes without loss of resolution, and are less susceptible to B0 inhomogeneity-related distortions than 2D-sequences. Contrast-enhanced T1-weighted images with fat suppression are helpful to suppress the bright signal of fat tissue of the skull base that might obscure the accuracy of tumor contouring and to discern postoperative changes. T2-weighted images can be sensitive in identifying brain parenchymal abnormalities, e.g. tumor infiltration and peritumoral edema; a cerebrospinal fluid (CSF) cleft between the lesion and the brain is often seen in benign extra-axial tumors as a T2-weighted crescent, whereas such clefts can be absent when aggressive tumors invade the brain parenchyma. Finally, the use of high-resolution 3D T2-weighted steady-state precession sequences, including three-dimensional Constructive Interference Steady State [3D-CISS] or Fast Imaging Employing Steady-state Acquisition [FIESTA], may be useful for improving the visualization the cisternal segments of cranial nerves.

For resected tumors, the treatment planning is based on postoperative MRI, although preoperative images may provide useful information regarding either the initial extent of disease or the identification of persistent brain infiltration after resection of aggressive tumors, e.g chordomas, atypical and malignant meningiomas. In addition, preoperative MRI is helpful to discern postoperative changes from tumor tissue, especially in patients who have undergone several prior surgeries. For planning purposes, MRI scans are subsequently fused with thin-slice non-contrast enhanced CT scans. Of note, CT scans may have a complimentary role in the imaging of skull base, specifically showing the pattern of bone involvement, e.g. hyperostosis and osteolysis, as well identifying intratumoral calcification better than MRI [30]. A contrast-enhanced CT is usually recommended only if MRI cannot be performed. Provided that a robust quality assurance (QA) protocol for registration of CT and MRI data sets for treatment planning is implemented and geometric distortion correction is applied, no additional margins would be required to ensure adequate target coverage to compensate for fusion uncertainties.

General target delineation strategy

The gross tumor volume (GTV) is defined as the visible lesion on MRI; typically, this is the contrast-enhancing lesion. The clinical target volume (CTV) is defined as the volume of tissue that contains the GTV and any microscopic disease and potential paths of microscopic spread. In general, additional margin expansion from GTV to CTV is unnecessary for benign skull base tumors; however, a small margin of 1–3 mm may be added to encompass potential areas of microscopic tumor infiltration, e.g the intracavernous portion of rapidly growing lesions. For specific histologies, such as atypical and malignant meningiomas or chordomas, large CTV margins in the range of 10–20 mm are frequently utilized to adequately cover the microscopic extent of disease, that may be reduced around natural barriers to tumor growth such as the skull.

The planning target volume (PTV) is defined as the margin accounting for both the internal and external uncertainties in treatment planning and delivery, including those arising from CT-MRI fusion and patient setup. No GTV-to-PTV margin is usually applied to invasive frame-based SRS. With the use of modern frameless SRS systems, either CyberKnife (CK) or dedicated LINAC technology (Novalis Tx™) [32–38], a sub-millimetric accuracy of target positioning has been reported; in clinical practice, a margin of 1–2 mm is generally used for GTV-to-PTV expansion in patients receiving frameless SRS, while a larger margin up to 3 mm is applied for those undergoing SRT; in this regard, each department should audit their setup results and apply the margins on the basis of their own measurements. When using conventionally fractionated 3D-conformal RT or intensity-modulated radiotherapy (IMRT), larger PTV margins of about 3–5 mm are required, being similar to those used for proton beam therapy. With the aim of decreasing the variability of clinical target volume delineation, it is important to develop a rigorous peer reviewed QA process at the departmental level [39]. All contouring steps should be supervised by an expert radiation oncologist. Before the planning process, an additional review done by other radiation oncologists is recommended to improve target volume delineation and to decrease inter-observer variability.

Organs at risk

The skull base region contains important endocrine, nervous, and vascular structures; then, a careful delineation of all organs at risk (OARs) including brain parenchyma, optic nerves and chiasm, brainstem, pituitary stalk, pituitary gland, cochleae, hippocampi, eyes, and lenses are essential to predict and hopefully prevent normal tissue injury. An example of OARs delineation on MRI in a patient with a skull base tumor is shown in Fig. 1. Definition of OARs delineated in Fig. 1 is summarized in Table 1. An atlas of brain OARs relevant to neuro-oncology has been recently created by the ESTRO taskforce “European Particle Therapy Network (EPTN)” and is available online on www.cancerdata.org [40]. Expansion of OARs to create a planning risk volume (PRV) for each OAR may be applied; the margin, as for the PTV, should reflect the accuracy of daily set-up. Overlaps between PRVs and PTV may occur; however, the delineation of the primary PTV margins should not be compromised and caution should be used when the reduction of the dose to the OARs may result in inadequate dose coverage of the PTV.

Techniques in skull base radiation oncology

Both SRS and SRT are employed for skull base tumors. Brain SRS, delivered in a single-or few (2–5) fractions, is typically performed using GK, CK, and LINAC-based SRS technologies. GK uses 192 radioactive cobalt-60 sources that are hemispherically arranged in a single internal collimation system via collimators to focus their beams to a center point. The tungsten collimators are organized into eight sectors of 24 sources each with three different apertures of 4, 8, and 16 mm, which deliver the radiation dose to the target using one or multiple isocenters depending on the size, shape, and location of lesions. Traditionally, patients who undergo GK are placed in a rigid stereotactic frame with a target accuracy <0.5 mm [32,33], although in its latest version (Icon GK) the dose can also be delivered as mask-based SRS.

The CK combines a compact 6-MV linear accelerator mounted on a robotic arm with 6 degrees of freedom. It uses adjustable

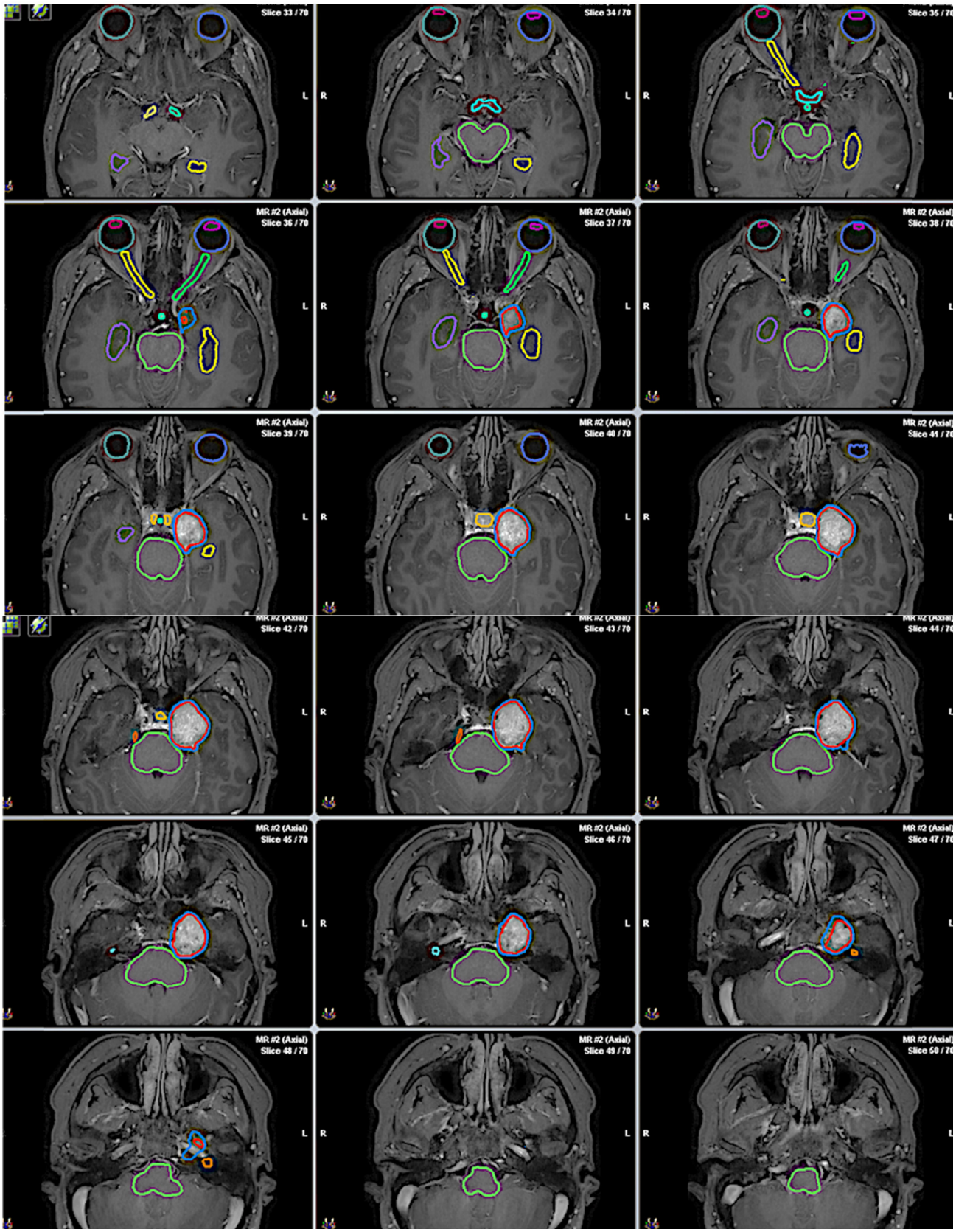

Fig. 1. An overview of target volumes and organs at risk (OARs) delineation of a skull base tumor (cavernous sinus meningioma) slice per slice is presented on post-contrast T1-weighted MRI sequences. The gross tumor volume (GTV) is presented in red and the planning tumor volume (PTV) in blue. The following OARs have been contoured: brainstem (green); optic chiasm (cyan); left optic nerve (lime green); right optic nerve (yellow); left eye (dark blue); right eye (aquamarine); right optic tract (lemon), left optic tract (light green); left lens (pink); right lens (dark red); pituitary gland (cheddar); pituitary stalk (turquoise); right hippocampus (purple); left hippocampus (gold); right fifth nerve (redorange); right cochlea (light blue); left cochlea (orange). (For interpretation of the references to colour in this figure legend, the reader is referred to the web version of this article.)

Table 1
Description of main organs at risk (OARs) contoured in the skull base tumor illustrated in Fig. 1.

OAR	Description
Left optic nerve (lime green; panels 3–6) and right optic nerve (yellow; panels 3–5). Thick, 2–5 mm	The optic nerve is delineated from the posterior edge of eyeball to the optic chiasm (panel 2–3). Visible on both MRI and CT, the latest useful for the relationsship with bony optic canal
Optic chiasm (cyan; panels 2–3). Thick, 2–5 mm	The optic chiasm is located in the suprasellar region (about 1 cm from the pituitary gland) anteriorly to the pituitary stalk. It is formed by the convergence of the optic nerves anteriorly (panel 3) and by the divergence of the optic tracts posteriorly (panel 1); laterally it is in contact/close proximiy to the Internal carotid artery. For a better delineation, coronal and sagittal images are recommended. The optic chiasm is better delineated on T1-weighted MRI sequences, visible also on CT
Right optic tract (lemon; panel 1) and left optic tract (light green; panel 1). Thick 2–5 mm	The optic tracts are visible posteriorly to the optic chiasm and anteriorly/laterally to the midbrain for 10–20 mm. Better delineation on T1-weighted MRI sequences, visible also on CT
Right (aquamarine) and left (dark blue) retina (posterior part of eyeball; panel 1–8). Thick, 2–3 mm	The retina is delineated on MRI and CT as the posterior part of the eyeball
Pituitary gland (cheddar; panels 7–10). Volume 0.25–0.5 cc	The pituitary gland lies on the sella turcica with a cranio-caudal dimension of 10–12 mm and bilaterally is bordered by cavernous sinuses. Visible on axial T1-weighted contrast-enhanced MRI. For a better delineation, coronal and sagittal images are recommended
Pituitary stalk (turquoise; panels 3–7). Thick 1–2 mm	The pituitary stalk has a lenght of 7–10 mm; it is delineated from hypothalamus (cranial limit) just behind the optic chiasm to the pituitary gland (caudal limit). For a better delineation, coronal and sagittal T1-weighted contrast-enhanced MR images are recommended
Brainstem (green; all panels)	The brainstem is seen on both MRI and CT. In craniocaudal direction, the midbrain, pons and medulla oblongata (up to the tip of C3 dens) are delineated. On panels 10 and 11, the right trigeminal nerve (fifth nerve) is delineated from the pons to the entrance of the nerve into Merckel's cave (redorange)
Right hippocampus (purple; panels 1–7) and left hippocampus (gold; panels 1–7). Volume, 2.5-4.0 cc	The hippocampus is constituted by grey matter and is easily distinguishable on T1-weighted MRI sequences. It is delineated as hypointense area medial to the curve of the temporal horn of the lateral ventricle (from panel 7), then continuing in the upward direction, bordered medially by the by the lateral edge of the quadrigeminal cistern (panel 1). Sagittal images can help OAR delineation
Right cochlea (light blue; panels 13–14) and left cochlea (orange; panels 15–16). Volume 0.5-0.6 cc	The cochlea is a spiral structure located in a bony cavity in the petrous portion of the temporal bone, anterior to the labyrinth, lateral to the internal auditory canal. It can be delineated on the basis of CT or MRI (better T2-weighted MR images) without inclusion of the semicircular canals (located laterally and cranially of the cochlea)

collimator cones ranging from 5 to 60 mm to generate highly conformal treatments with up to 200 overlapping beams which are delivered non-isocentrically to the target [41–43]. As for other LINAC-based SRS systems, patients are fixed in a thermoplastic mask and submillimeter target positioning accuracy is achieved with the use of regular high-resolution kV imaging acquired throughout the treatment.

With LINAC-based SRS, doses are delivered through multiple fixed beams or dynamic conformal arcs using either circular collimators or micro-multileaf collimators (MLC) with a leaf width of between 2.5 and 5 mm. Dose conformity is improved using IMRT and volumetric-modulated arc therapy (VMAT) techniques [44]. Patients are usually immobilized in a high precision frameless stereotactic mask fixation system and submillimeter accuracy of patient positioning in the treatment room is achieved using modern image guided radiation therapy (IGRT) technologies, such as orthogonal x-rays (ExacTrac®Xray 6D system) or cone beam CT (CBCT) [34–38].

For patients with large complex skull base tumors receiving conventionally fractionated SRT, IMRT and VMAT planning techniques are increasingly being used over 3D conformal RT because of its better target coverage and OARs sparing, although at the cost of larger volumes receiving low dose radiation. Precise immobilization and improved patient positioning can be achieved using sophisticated immobilization and image guidance systems as seen for LINAC-based SRS. Regardless of the used technique, strict protocols for QA must be followed since SRS and SRT require levels of precision and accuracy that surpass the requirements of 3D conformal RT and IMRT techniques.

Particle therapy, including protons and carbon ions, have been employed for skull base tumors using either fractionated RT or SRS [15,45–48]. A physical advantage of protons over photons is that they deposit most of their energy at the end of their range, with very little exit dose beyond the target volume. This narrow region of energy deposition is known as the Bragg peak and it may allow for a reduction in integral dose delivered to the surrounding normal tissues. Currently, there are two types of proton therapy delivery: passively scattered and pencil beam proton therapy. In passive scattering, a spread-out Bragg peak is generated by modulations of multiple mono-energetic beams to ensure a uniform does distribution across the target through a single or double scattering, the latter required for larger volumes. Dose conformation is achieved through the use of range shifter wheels and patient-specific apertures and compensators [49,50]. In active scanning (often called pencil beam scanning or spot scanning), proton dose dosimetry optimization can be achieved using narrow pencil proton beams, with a near monoenergetic Bragg peak, superposition of which constitutes the treated volume [51–53]. Intensity modulated proton therapy (IMPT) represents an advanced pencil-beam delivery optimization strategy; using this proton beam technology, both the scanning speed and the intensity of the beam are modulated to improve the PTV dose homogeneity and conformity, thus minimizing the dose delivered to OARs. Although different techniques and dose fractionation schedules can be used for treating skull base tumors, GTV and CTV target delineation strategies remain similar.

Planning details

The overall goal of radiation treatment planning is to ensure the optimal coverage of the target with the prescription dose while respecting all the OARs dose constraints. Depending on the technique, dose is prescribed to the 40–95% isodose surface. For LINAC-based and CK SRS treatments, the dose is typically prescribed to 70–80% isodose [21,54]. This is because the dose gradient falls off most quickly outside the target, between the 80% and 40% isodose surfaces [55]. Therefore, prescribing in this range minimizes the integral dose to all normal tissues, therefore affording the most OAR sparing. For multiple isocenter plans, this optimal surface shifts to the 40–50% isodose surface and can be extended to isodose surfaces as low as the 40% isodose surface, as is often the case in GK plans [56]. Prescription isodoses are typically higher when larger skull base tumors are treated with hypo- or conventional fractionation.

The risk of toxicity following irradiation of skull base tumors is influenced by different factors, including the total dose, dose per fraction, and the volume of normal tissue irradiated at high doses. A summary of dose/volume data and clinical risk estimates for central nervous system (CNS) structures following conventionally fractionated RT and SRS, based on a combination of clinical observations and reviews, is presented in Table 2 [57–73]. A recent consensus report of OAR dose constrains in neuro-oncology has been recently published by the European Particle Therapy Network of ESTRO with the aim to create a model-based approach comparing photon and proton beam irradiation [74].

Target volume definition for specific indications

Pituitary tumor

Transsphenoidal surgery is the first-line treatment for most pituitary tumors, either nonfunctioning or secreting tumors, such as ACTH- and GH-secreting tumors. Radical resection is achieved in a significant proportion of patients with a low incidence of peri- and post-operative complications [2,75–78]. Based on recent guidelines, RT is generally used in patients with large residual or recurrent pituitary tumors [4,5,12]. The reported local control of large retrospective series following either SRS or SRT [79] is in the range of 90–95% at 5–10 years, with normalization of hormone excess observed in about 50–60% of secreting pituitary adenomas; the time in reaching normalisation is related to the initial hormone level. Dose and fractionation are usually chosen on the basis of the type, size and location of the tumor. In current clinical practice, single-fraction SRS at doses of 13–16 Gy and 16–25 Gy is a feasible approach to patients with non-functioning and secreting pituitary adenomas less than 2.0–2.5 cm in size at safe distance from the optic chiasm (maximum point dose less than 8–10 Gy; see Table 2), respectively. Few studies report on fractionated SRS, usually 21 Gy in 3 fractions or 25 Gy in 5 fractions, showing tumor control rates consistent with that observed after single-fraction SRS [79,80]. For larger lesions and/or those involving the anterior optic pathway, fractionated RT, including either SRT or IMRT, is usually recommended. Doses of 45–50.4 Gy are typically delivered in 25–28 fractions of 1.8–2.0 Gy per fraction, with higher doses used when treating secreting pituitary adenomas; doses up to 54 Gy may be used for large aggressive pituitary tumors and carcinomas [5,81].

The GTV is defined as the visible lesion on MRI. Target delineation should be performed using pre- and postcontrast-enhanced isotropic 3D T1-weighted sequences with 1 mm slice thickness. Preoperative and contrast-enhanced T1-weighted images with fat suppression may be helpful to discern postoperative changes from the tumor (including fat or biomaterial apposition), especially in patients who have undergone several surgeries. When MRI is contraindicated, a contrast-enhanced thin-slice CT through the pituitary region should be performed before and after contrast administration. Additional margin expansion from GTV to CTV is unnecessary; however, a margin of 2–3 mm may be added in case of invasive and aggressive pituitary tumors to encompass all potential areas of microscopic tumor infiltration, e.g. fast-growing tumors invading the cavernous sinus. For fixed-frame SRS, no GTV-to-PTV margin is generally necessary, whereas an additional safety margin of around 1–3 mm is usually used for frameless SRS and SRT depending on institutional practice. If advanced image guided techniques are not available, larger margins up to 5 mm should be employed. OARs include optic nerves and chiasm, brainstem, pituitary stalk, pituitary gland, cochleae, hippocampi, normal brain, eye, and lenses.

Meningioma

Intracranial meningiomas represent about one third of all primary brain tumors with an estimated annual incidence of approximately 6 per 100.000 people, generally increasing with age. According to the World Health Organization (WHO) classification scheme [82], meningiomas are histologically characterized as benign (grade I), atypical (grade II), or malignant (grade III). Typical characteristics of grade II meningiomas are a mitotic count of 4–19 per HPF and/or brain invasion. Grade III meningiomas are characterized by elevated mitotic activity (20 or more per HPF) or frank anaplasia. Surgery is the treatment of choice for the majority of symptomatic and enlarging meningiomas, with the aim of alleviating symptoms, relieving mass effect, and providing histology. Complete resection of the tumor and any involved dura or bone is the gold standard for meningioma and is associated with long term local control in more than 80% of patients at 5–10 years [3,83].

RT is usually employed in patients with residual or recurrent benign meningiomas following surgical resection, for those with unresectable tumors or not amenable to surgery, and with atypical

Table 2
Summary of normal tissue constrains using standard fractionated RT (2 Gy per fraction) and SRS (1-5 fractions).

Organ	Type of radiation	Dose constraint (toxicity rate)	Type of toxicity	References
Brain	Standard fractionation	Dmax <60 Gy to whole organ (<3%)	Symptomatic necrosis	[57,60,63,72,73]
	Single-fraction SRS	12 Gy to <5–10 ml (<10-20%)		
	3-fraction SRS	18 Gy (6 Gy/fx) to <26 ml (3%)		
Brainstem	Standard fractionation	Dmax <54 Gy to whole structure (<5%)	Permanent cranial deficit or necrosis	[57,60,63,65]
	Single-fraction SRS	Dmax <12.5 Gy (<5%; 1% if to 1/3 of brainstem		
	3-fraction SRS	Dmax 18 Gy (6 Gy/fx) to <1 ml (<3%)		
	5-fraction SRS	Dmax 26 Gy (5.2 Gy/fx) to <1 ml (<3%)		
Optic nerve/chiasm	Standard fractionation	Dmax <55 Gy to whole structure (<3%)	Optic neuropathy	[57,58,66,69]
	Single-fraction SRS	Dmax <8 Gy (<3%), Dmax 8-12 Gy (<10%)		
	3-fraction SRS	19.5 Gy (6.5 Gy/fx) (<3%)		
	5-fraction SRS	Dmax 25 Gy (5 Gy/fx)(<3%)		
Cochlea	Standard fractionation	Mean dose ≤45 Gy to whole structure (<15%)	Hearing loss	[57,60,61]
	Single-fraction SRS	Dmax ≤14 Gy (<25%)		
	3-fraction SRS	Dmax 20 (6.67 Gy/fx) (<3%)		
	5-fraction SRS	Dmax 27.5 (5.5 Gy/fx) (3%)		
Pituitary gland	Standard fractionation	Dmax ≤45 Gy to whole gland (20-40% at 5 years)	Hypopituitarism	[59,64,67,68,70]
	Single-fraction SRS	Dmax <15 Gy (2-30% at 5 years)		
Hippocampus	Standard fractionation	Dmax ≤7.3 Gy to 40% of structure (impairment in Wechsler Memory Scale-III Word List delayed recall)	Memory impairment	[71]
Medulla Oblongata	Standard fractionation	Dmax 54 Gy (1%) and 61 Gy (10%)	Myelopathy	[57,60,62]
	Single-fraction SRS	Dmax 13 Gy (1%)		
	3-fraction SRS	Dmax 22.5 Gy (6.67 Gy/fx) (1%)		
	5-fraction SRS	Dmax 30 Gy (6 Gy/fx) (1%)		

RT, Radiation Therapy; SRS, Stereotactic radiosurgery; Dmax, maximum dose.

or malignant tumors [3,11,13]. For benign meningiomas, local control rates after fractionated RT and SRS ranges from 85% to 95% at 5–10 years, with a reported low neurological and endocrinological toxicity [11,13,84–86]. Similar results have been shown after proton beam RT [17,87,88]. Typical doses used for SRS are 13 to 15 Gy given in a single fraction and 21–25 Gy given in three to five fractions. As for other skull base tumors, fractionated schedules with doses of 50–55 Gy in 25–33 daily fractions of 1.67–2.0 Gy, commonly 54 Gy at 1.8 Gy per fraction, are employed in the treatment of tumors larger than 3 cm in size or involving sensitive brain regions, i.e. brainstem or optic apparatus, while single-fraction SRS has been widely used to treat smaller lesions away from the optic chiasm.

Using doses of 54–60 Gy in 30–33 daily fractions of 1.8–2.0 Gy, two prospective phase II trials published by the Radiation Therapy Oncology Group (RTOG 0539) and the European Organisation for Research and Treatment of Cancer (EORTC) have shown progression-free survival rates of about 94% and 89%, respectively, at 3 years [89–91]. Although these trials suggest progression-free survival benefits of fractionated RT in patients with atypical meningiomas at three years with acceptable toxicity, the question if early adjuvant RT may reduce the risk of tumor recurrence after gross total surgical resection of a WHO grade II meningioma remains unanswered. A phase III intergroup trial is currently recruiting patients with atypical meningiomas who are randomized between observation and adjuvant treatment following surgery [92]. RT remains the treatment of choice in all malignant meningiomas, regardless of the type and extent of surgery although evidence of benefit is not clear.

For benign meningiomas, the GTV is generally defined as the visible lesion on contrast-enhanced T1-weighted MR images with 1–2 mm slice thickness. An example of target delineation for a cavernous sinus meningioma is given in Fig. 1. For atypical (Grade II) and malignant (Grade III) meningiomas, the GTV delineation should be based on the resection cavity (if available) plus any residual tumor without inclusion of the perilesional edema. Additional images that can help to improve target delineation include T2-weighted high-resolution gradient and fast spin echo sequences with and without fat suppression, and fluid attenuated inversion recovery (FLAIR) sequences. Specifically, T2-weighted sequences can also be useful to assess the extent of peritumoral edema and dural tail abnormalities [93,94]. In addition, extra-axial growth can be verified on T2-weighted images by cerebrospinal fluid (CSF) cleft interposed between the tumor and the parenchyma. CT is valuable for the detection of calcification of varying degrees within the tumor and hyperostosis of adjacent bone. In selected cases, PET imaging mainly with DOTATOC- or DOTANOC-tracers has shown to improve target volume definition, e.g. patients with large tumors infiltrating the parapharyngeal soft tissues or for those located in the bony structures which are difficult to be distinguished on MRI and CT [95–102].

The majority of meningiomas are durally based, and the question is whether the dural tail, which is the linearly enhanced dura trailing off from the meningioma for several millimeters, should be included or not in the GTV. Dural tail, that can be accurately identified in post-gadolinium T1-weighted images [93,94], is typically composed entirely or almost entirely of hypervascular dura [83,103–105] with microscopic clusters of meningioma that have been only occasionally observed in the dura adjacent to the tumor [106]. Although the issue remains matter of debate, there is no clear evidence that recurrences are more likely to occur within the dural tail than any other portion of dura next to the main tumor mass [107–109]. According to RTOG 0539 and EORTC 1308 trials, only clearly thickened dural tail should be considered as target and included in the GTV (Fig. 2); in contrast, linearly enhanced dura and non-enhancing but thickened dura trailing off the tumor would not be included in the GTV. The same goes for the hyperostotic bone; only directly invaded bone and clearly hyperostotic bone should be included in the GTV using a CT bone window setting to improve target delineation (Fig. 3), as applied for EORTC 1308 and RTOG 0539 trials. For meningiomas characterized by diffuse and extensive dural involvement (so called "en plaque meningiomas), usually with extracranial extension into calvarium, orbit, and soft tissues, all dural thickening and enhancement should be included in the GTV.

In general, additional margin expansion from GTV to CTV is unnecessary for benign meningiomas; however, a small margin of few millimeters may be added to encompass potential areas of microscopic tumor infiltration in case of rapidly growing tumors, e.g the intracavernous portion or the proximal region of the dural tail (avoiding extensive coverage of the distal portion). For Grade II and III meningiomas, the CTV is defined as the GTV plus a 1–2 cm margin and might include the pre-operative tumour bed, the peritumoural edema, hyperostotic bone changes, and the dural enhancement or thickening as seen at diagnosis; margins may be smaller (3–5 mm) around natural barriers to tumor growth such as the skull, and into surrounding brain parenchyma unless there is evidence of invasion.

Depending upon localization method and reproducibility, an institution-specific margin up to 5.0 mm is usually added to the CTV to generate the PTV. As for other skull base tumors, OARs have to be defined through MR (e.g., optic chiasm and nerves, pituitary gland and stalk, brainstem, carotid artery, hippocampi, lacrimal gland) and CT scan (lens, cochlea) in all plans.

Craniopharyngioma

Surgery is the initial treatment modality for most patients with a craniopharyngioma; complete resection is associated with a 5-year tumor growth control of 70–90% in adult and pediatric series, although aggressive surgical management is associated with a high risk of complications [110–114], particularly relating to hypothalamic damage. Limited surgery followed by radiation is an alternative to aggressive surgical treatments associated with comparable outcome and lower risk of long term sequelae [112,115–119].

For incompletely resected and recurrent tumors, conventionally fractionated postoperative RT is the recommended treatment. Using doses of 50–55 Gy in 25–33 daily of 1.67–2.0 Gy with either photons or protons, several large retrospective series report tumor control rates of 85–95% and survival rates of 90–100% at five years [15,17,120–123]. Compared with 3D conformal RT, IMRT-based stereotactic techniques and IMPT can offer improved dose conformality and reduced dose to adjacent normal structures [15,17]. SRS may represent an alternative treatment option in selected patients with small residual or recurrent craniopharyngiomas. Both single-fraction SRS up to18 Gy and fractionated SRS (20–25 Gy in 3/5 fractions) have been employed in selected patients with a small tumor away from the optic chiasm; few retrospective series with limited number of patients report tumor control rates of 60 to 80% at five years, with long-term toxicity occurring in 3–7% of patients, mainly visual deterioration [124–129].

The GTV is defined as the visible lesion on post-contrast T1-weighted and T2-weighted MRI sequences with a 1–2 mm slice thickness to ensure the accuracy of target delineation. The solid portion of craniopharyngiomas is more precisely contoured using the contrast-enhanced 3D T1-weighted images, whereas fast spin-echo T2-weighted images with and without fat suppression allow for better visualization of cystic components of the tumor. The GTV has historically been expanded by a margin of 10–20 mm to generate the CTV and the PTV, given less reliable immobilization and image guidance; however, margins have progressively reduced. Currently, some institutions include a 3–5 mm

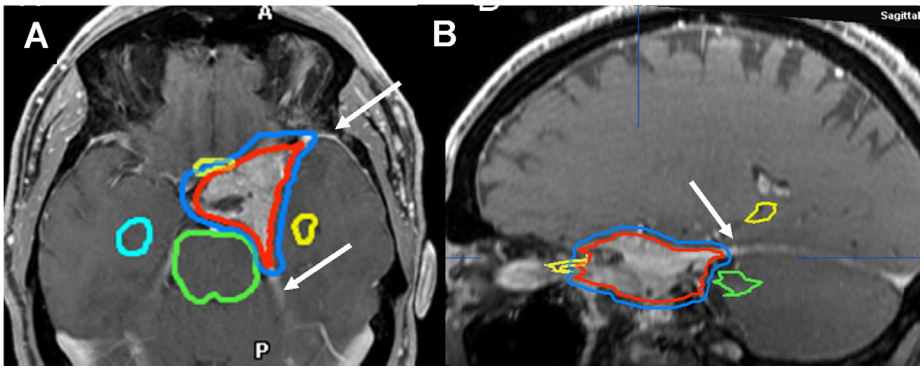

Fig. 2. Example of delineation of the dural tail for a skull base meningioma on axial (A) and sagittal (B) post-contrast T1-weighted MRI. Only thickened dural tail was included in the GTV (blue contour); in contrast, linearly enhanced dura (white arrows) was not included in the GTV. (For interpretation of the references to colour in this figure legend, the reader is referred to the web version of this article.)

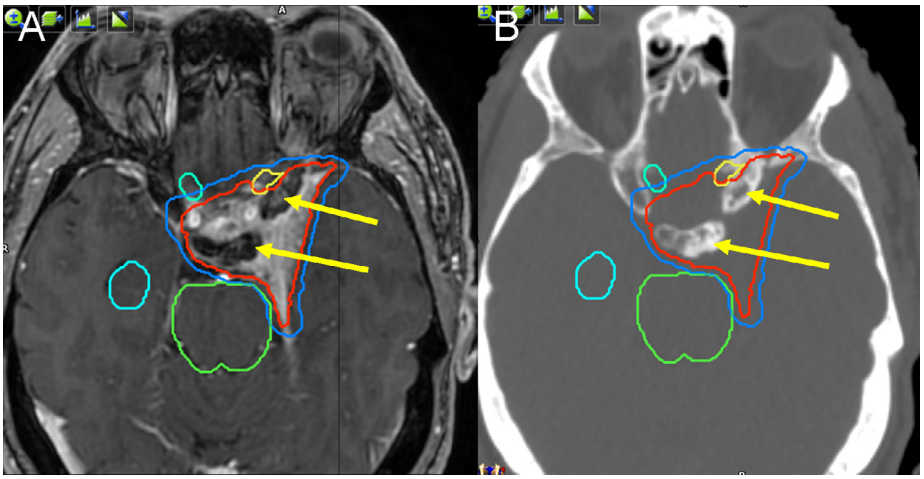

Fig. 3. Example of bony hyperostosis associated with a skull base meningioma on MRI (A) and CT (B) images. All areas of hyperostotic bone (yellow arrows) and potential bony tumor invasion were included in the gross tumor volume (GTV, red contour) using a CT bone window setting to improve target delineation. (For interpretation of the references to colour in this figure legend, the reader is referred to the web version of this article.)

GTV-to-CTV margin to take into account potential microscopic areas of tumor infiltration and changes of cystic components of the tumor during the treatment that may occur in up to 40% of patients [130]; as for other skull base tumors, margins can be reduced at sites where tumor invasion is unlikely, e.g. skull base bones. The surgical report provides additional information that may help to identify all areas of adhesion noted intraoperatively into the CTV. Of note, few series have shown an excellent long-term control after fractionated SRT using smaller or no GTV-to-CTV expansion, then supporting the noninfiltrative nature of this tumor and the use of a reduced GTV-to-CTV margin [120,122]. Because a challenging component of craniopharyngioma management is the potential for cystic growth, a close surveillance imaging during the treatment is mandatory when reduced margins are used. For OARs delineation and dose constraints see above (Fig. 1). As for other tumors, PTV margins depends on institutional practice and used radiation technique.

Vestibular schwannoma

Vestibular schwannomas originate from the Schwann cells surrounding the eighth cranial nerve. Generally, they are benign, slow growing lesions and are associated with 1–3 mm growth per year [131–133]. Unilateral vestibular schwannoma is the most common form (95%); neurofibromatosis-2 (NF2) accounts for 5% of all vestibular schwannomas and typically affects the VIII nerve bilaterally and young people [134,135]. Common symptoms include hearing loss or impairment, dizziness, tinnitus, and gait uncertainties.

Current treatment options for vestibular schwannoma include observation, surgical resection, SRS, and SRT. The choice of treatment depends on clinical presentation, tumor size, and expertise of the treating center. Small lesions which are asymptomatic can be observed with serial MRI scanning and audiological monitoring without any tumor-directed treatment [6,136]. Surgery is considered as the primary treatment to remove a symptomatic lesion or potentially life-threatening mass effect, although the treatment may also be considered for smaller tumors [6,137,138]. Gross total resection or near total resection is associated with local control rates of 80–90% [137–142]; in experienced surgical centers, the probability of hearing preservation in patients with small lesions and normal hearing is about 50–75% and 25–50% after 5 and 10 years [139,140], respectively, and the risk of persisting facial palsy is between 3% and 15%. [141].

RT is a safe and effective treatment for vestibular schwannomas; depending on the size of the lesion, it can be applied as SRS or fractionated SRT with comparable local control of 90–99% at

5 years, hearing preservation rates of 50–79%, facial nerve preservation rates of 95–100%, and trigeminal preservation rates of 80–99% [135,143–155]. Dose of single-fraction SRS should be in the range of 12–13 Gy. For patients receiving conventional fractionation, total doses ranging from 45 to 54 Gy given in 25–30 daily fractions of 1.8–2.0 Gy are currently recommended [6]. Hearing preservation rates are in the range of 60–90%, with patients with useful hearing prior to RT having the highest chance to fully preserve their hearing function [152–155]. Few retrospective series indicate that hypofractionated schedules may represent an effective treatment option for large vestibular schwannomas, typically 18 Gy in 3 fractions or 25 Gy in 5 fractions [156,157].

For GTV delineation, thin slice CT and MRI with and without contrast enhancement are recommended. The GTV is represented by the lesion visible on isotropic contrast-enhanced 3D T1-weighted sequences with 1 mm slice thickness. Additional sequences are represented by high resolution 3D T2-weighted sequences (e.g. CISS/FIESTA) may improve the visualization of cisternal segments of the lower cranial nerves and their relationship with the tumor. For contouring, bony CT windows are helpful since the enlargement of the vestibular canal can be visible representing the tumor volume. For frame-based SRS, no additional safety margin is necessary as precise positioning is established. With frameless SRS and SRT, a GTV-to-PTV safety margin of around 1–3 mm can be necessary depending on immobilization and IGRT techniques used at different institutions.

Chordoma/Chondrosarcoma

Chordomas and chondrosarcomas are rare, locally aggressive tumors occurring in one third of cases in the base of the skull. The mainstay of treatment is maximal tumor debulking. En bloc resection is the recommended treatment with 5-year local recurrence free-survival rates of more than 50% [1,158–160]; however, en bloc resection with R0 margins for skull base chordomas and chondrosarcomas (negative microscopic margin of 1 mm or greater of normal tissue around the tumor) is very rarely achievable, despite major advances in cytoreductive surgical interventions. Surgery should be practiced in referral centers, since the quality and extent of surgery are the principal determinants of outcome, together with tumor size, quality of RT, and patient age [161,162].

Proton beam therapy has been traditionally used for the radiation treatment of chordomas with doses of 72–76 Gy achieving a local tumor control between 60% and 81% at 5 years [7,162–164]. Moderate hypofractionation with 16–22 fractions of 3–4·2 GyE per fraction is feasible using carbon ions [1]. Using photon radiation, a few studies have reported 5-year local control rates of 50–76% after conventionally fractionated SRT using doses up to 70 Gy at 1.8–2.0 Gy per fractions and GK SRS using marginal doses of 13–20 Gy [15,165–170]. Using similar doses, retrospective series have reported better local control rates in the range of 94–100% at 10 years for chondrosarcomas [8,171], although it is questionable if these patients need high-dose radiation, as tumors with good prognostic factors (i.e. small residual tumors, young age, no brainstem/optic apparatus abutment) rarely recur and treatments can carry significant risk of radiation-induced toxicity, including but not limited to temporal lobe necrosis and optic neuropathy.

For the target delineation of these challenging tumors, the GTV is usually delineated as the tumor remnant observed on MRI sequences with 1–2 mm slice thickness, including T1-weighted, T2-weighted, and contrast-enhanced T1-weighted imaging fused to the planning CT. Even though there is no unanimous consensus on optimal target delineation of these tumors, it is key to include comprehensive margins in the delineation process, as inadequate 'radiosurgical' margin reduction can be associated with a higher rate of treatment failure. The CTV should encompass all potential areas at risk of microscopic spread of disease and is typically based on preoperative tumor volume and postoperative residual tumors and resection margins.

In many proton centers, two distinct CTV volumes receiving different doses are applied: the primary CTV (CTV1, 54 GyRBE) is usually defined by preoperative tumor volume with an anisotropic margin of 10–20 mm plus the residual tumor and surgical resection margins. Normal structures previously compressed by the tumor that re-expand after surgery are not included in the CTV1, e.g. brainstem, chiasm, temporal lobe parenchyma, or pharynx (in case of tumor extension to the cervical spine). Similarly, peritumoral edema, as seen in cases of initial compression of the temporal lobe, does not require inclusion in the CTV. The surgical tract is not comprehensively treated in skull base chordomas since this delineation strategy would result in a substantial increase of normal tissue irradiation, and bearing in mind that surgical pathway failure after surgical seeding is rare (i.e. 1–2%) [34,172]. For patients receiving a transsphenoidal approach, the posterior part of residual sphenoid sinus is routinely included in the CTV1. A second CTV (CTV2) receiving a higher boost-dose of radiation (74–76 GyRBE for chordoma, 70–72 GyRBE for chondrosarcoma) should comprise the residual tumor with a geometrical expansion of 5–10 mm (reduced around natural barriers to tumor growth) plus the resection margins at higher risk of residual disease. In case of macroscopically radical resection, CTV2 is limited to the resection margins. Depending on radiation techniques and available technology, a variable CTV-to-PTV margin up to 5 mm is applied, with protons usually requiring larger margins than photon stereotactic techniques.

Conclusions

More accurate and uniform target delineation guidelines for skull base tumors should help to promote equality and improvement of outcomes. A summary of recommended imaging modalities for target volumes delineation and dose fractionation using either fractionated RT or SRS for different skull base tumors is reported in table 3. While recognising that there is a range of approaches to defining the target volume of the different tumor entities, the ESTRO ACROP guideline committee proposes the following pragmatic algorithm:

- Immobilization with a fixed or relocatable frame or a closely fitting thermoplastic mask system, planning CT with 1–2 mm slice thickness.
- Fusion with MRI obtained at the time of radiation treatment, usually isotropic contrast-enhanced 3D T1-weighted sequences with 1 mm slice thickness. Other examinations, including preoperative MRI, unenhanced T1-weighted MRI, and high-resolution 3D T2-weighted MRI sequences may allow more precise target delineation.
- GTV defined as the T1-weigted contrast-enhancing lesion. For atypical and malignant skull base tumors, e.g. chordomas and atypical and malignant meningiomas, GTV includes the resection cavity (if available) plus any enhancing residual tumor.
- No margin around the GTV should be applied to generate the CTV in benign tumors, but this can be edited to take into account possible microscopic disease, e.g. cavernous sinus or brain parenchyma in rapidly growing, invasive tumors. A variable GTV-to-CTV margin of 1–2 cm is applied in aggressive and malignant tumors.
- No CTV-to-PTV margin is usually necessary for invasive frame-based SRS; 1–2 mm margin expansion is generally used in patients receiving frameless SRS and up to 3 mm for those undergoing SRT depending on accuracy of patient immobilization, positioning and monitoring systems. If IGRT techniques

Table 3
Summary of imaging modalities for target volumes delineation and dose/fractionations for skull base tumors.

Tumor type	WHO grading	Imaging for target delineation	Gross Tumor Volume (GTV)	Clinical Tumor Volume (CTV)	Planning Target Volume (PTV)	Dose and fractionation
Pituitary tumor	Typical adenoma or high-risk adenoma (rapid growth, radiological invasion, high Ki-67 proliferation index)	Isotropic pre- and post-contrast-enhanced 3D T1-weighted MRI sequences with 1 mm thick slices	Visible lesion on MR images	Margin expansion from GTV-to-CTV is unnecessary for typical adenoma; a GTV-to-CTV margin of 2–3 mm may be added in aggressive pituitary tumors and carcinomas	For fixed-frame SRS, no additional safety margin is necessary; for frameless SRS and SRT, a GTV-to-PTV margin of 1–3 mm is usually used	16–25 Gy using single-fraction SRS; 21–25 Gy in 3–5 fractions using fractionated SRS; 45–50.4 Gy at 1.8–2.0 Gy per fraction using fractionated RT (large tumors involving the optic apparatus). Higher doses up to 54 Gy for high-risk tumors)
Meningioma	WHO grade I	Isotropic post-contrast-enhanced 3D T1-weighted MRI sequences with 1 mm thick slices and T2-weighted images. PET-Imaging with DOTATOC- or DOTANOC-tracers may improve GTV delineation in selected cases	Visible lesion on MR images; only thickened dural tail should be included in the GTV (not linearly enhanced dura and non-enhancing tickened dura)	Margin expansion from GTV-to-CTV is usually unnecessary	For fixed-frame SRS, no additional safety margin is necessary; for frameless SRS and SRT, a GTV-to-PTV margin of 1–3 mm is usually used	13–15 Gy using single-fraction SRS; 21–25 Gy in 3–5 fractions using fractionated SRS; 50–55 Gy at 1.67–2.0 Gy per fraction using fractionated RT (usually large tumors involving the optic apparatus)
	WHO grade II WHO grade III	Isotropic pre- and post-contrast-enhanced 3D T1-weighted sequences with 1 mm thick slices and T2-weighted images. PET-Imaging may improve GTV delineation in selected cases. CT can be useful for the detection of calcification within the tumor and hyperostosis of adjacent bone	Tumor bed on postoperative contrast-enhanced T1-weighted MR images with inclusion of any residual nodular enhancement. Clearly hyperostotic bone should be included in the GTV	The CTV is defined as the GTV plus 1–2 cm margins and should include the pre-operative tumor bed, peritumoral edema, hyperostotic bone changes, and dural enhancement or thickening. Smaller margins (5–10 mm) around natural barriers to tumor growth, such as the skull, and into surrounding brain parenchyma unless there is evidence of invasion	A CTV-to-PTV margin up to 5.0 mm are usually added (institution specific)	54–60 Gy in 30 daily fractions of 1.8.2.0 Gy is recommended; SRS 14–16 Gy may be an option for small recurrent tumors
Craniopharyngioma	WHO grade I	Isotropic pre- and post-contrast T1-weighted and T2-weighted MRI sequences with 1 mm thick slices.	Visible lesion on contrast-enhanced T1-weighted MR images. T2-weighted fast spin-echo technique may allow for better visualization of cystic components of the tumor.	GTV-to-CTV expansion is unnecessary as for other non-infiltrative tumors,; however, some institutions use 3-5 mm GTV-to-CTV margin with fractionated RT.	For fixed-frame SRS, no additional safety margin; for frameless SRS and SRT, a GTV-to-PTV margin of 1-3 mm is usually used according to Institutional practice.	50-55 Gy at 1.67-1.8 Gy per fraction; single-fraction SRS (12-18 Gy) or fractionated SRS (21-25 Gy in 3/5 fractions for selected patients with small tumors away from optic chiasm.
Vestibular Schwannoma	WHO grade I	Isotropic pre- and post-contrast T1-weighted and T2-weighted MRI sequences with 1 mm thick slices. Additional images include high resolution 3D T2-weighted sequences (e.g. CISS/FIESTA)	Visible lesion on contrast-enhanced T1-weighted MR images. High resolution 3D T2-weighted sequences may improve visualization of the target and cranial nerves	Margin expansion from GTV to CTV is usually unnecessary	For SRS, no additional safety margin is necessary; with frameless SRS and SRT, a GTV-to-PTV safety margin of 1–3 mm is usually used	12–13 Gy using single-fraction SRS; 18–25 Gy in 3–5 fractions using fractionated SRS; 45–54 Gy at 1.8–2.0 Gy per fraction using fractionated RT (large tumors, e.g. >3 cm in size)
Chordoma	Well-	Isotropic pre- and	Visible lesion on MR	The CTV is tipically	A CTV-to-PTV margin	With proton

(*continued on next page*)

Table 3 (*continued*)

Tumor type	WHO grading	Imaging for target delineation	Gross Tumor Volume (GTV)	Clinical Tumor Volume (CTV)	Planning Target Volume (PTV)	Dose and fractionation
Chondrosarcoma	differentiated or dedifferentiated (chordomas) WHO grade I–III (chondrosarcoma)	post-contrast-enhanced 3D T1-weighted sequences with 1 mm thick slices and T2-weighted images	images	based on preoperative tumor volume and postoperative residual tumors/resection margins. Two different CTVs generally employed: – CTV1, preoperative tumor volume with anisotropic margins of 1–2 cm plus the residual tumor and surgical resection margins (54 Gy); – CTV2 encompassing the residual tumor with an expansion of 5–10 mm plus resection margins (74–76 Gy)	up to 5 mm is applied, with protons usually requiring larger margins than photon stereotactic techniques	irradiation, 72–76 GyRBE at 1.8–2.0 Gy per fraction (use 70–72 GyRBE for chondrosarcoma); with photon irradiation, fractionated RT at doses of 66–70 Gy at 1.8–2.0 Gy per fraction; SRS at doses of 13–20 Gy

are not available, larger margins up to 5 mm should be employed.

- Single-fraction SRS, fractionated SRS (2–5 fractions) or conventionally fractionated SRT are commonly used, depending on tumor types, target volumes and involvement of critical OARs.
- Conventionally fractionated RT using IMRT and VMAT technology for improving dose conformity is usually delivered at doses of 45–60 Gy in 25–33 daily fractions of 1.67–2.0 Gy according to different tumor types and grade (higher doses reserved for aggressive tumors, e.g. atypical and malignant meningiomas); SRS doses of about 13–22 Gy in single fraction and 21–25 Gy in 3–5 fractions are typically utilized according to the different histologies.
- Doses up to 74–76 Gy in 1.8–2.0 Gy fractions for chordomas; lower doses for chondrosarcomas.

Abbreviations

ACROP, Advisory Committee on Radiation Oncology Practice
ASTRO, American Society for Radiation Oncology
CBCT, Cone-beam computed tomography
CISS, Constructive Interference Steady State
CK, CyberKnife
CNS, Central nervous system
CT, Computed tomography
CTV, Clinical target volume
EORTC, European Organisation for Research and Treatment of Cancer
ESTRO, European Society for Radiotherapy & Oncology
FIESTA, Fast Imaging Employing Steady-state Acquisition
FLAIR, Fluid-attenuated inversion recovery
GK, Gamma Knife
GTV, Gross tumor volume
LINAC, Linear Accelerator
IGRT, Image-guided radiotherapy
IMPT, Intensity-modulated proton beam therapy
IMRT, Intensity-modulated radiotherapy
MRI, Magnetic resonance imaging
OARs, Organs at risk
PET, Positron-emission tomography
PTV, Planning tumor volume
PRV, Planning organ at risk volume
RT, Radiation therapy
RTOG, Radiation Therapy Oncology Group
SRS, Stereotactic Radiosurgery
SRT, Stereotactic Radiotherapy
VMAT, Volume Modulated Arc Therapy
MPRAGE, Magnetization prepared rapid acquired echoes
3D FLASH, Three-dimensional fast low angle shot
3D FGRE, Three-dimensional fat-suppressed 3D fast gradient echo
3D FSPGR, Three-dimensional fat-suppressed spoiled gradient echo
3D TFE, Three-dimensional turbo field echo

Preparation of the guideline

The guideline was prepared following the ESTRO procedure policy for guidelines. GM and SC coordinated the guideline panel and drafted the manuscript. BB, MB, AB, MB, LF, AF, UG, ALG, FLL, MN, TN, IP, DCW, and CB were part of the expert panel and contributed to the development, preparation and shaping of the manuscript. All authors read and approved the final manuscript.

Disclaimer

ESTRO cannot endorse all statements or opinions made on the guidelines. Regardless of the vast professional knowledge and scientific expertise in the field of radiation oncology that ESTRO possesses, the Society cannot inspect all information to determine the truthfulness, accuracy, reliability, completeness or relevancy thereof. Under no circumstances will ESTRO be held liable for any decision taken or acted upon as a result of reliance on the content of the guidelines.

The component information of the guidelines is not intended or implied to be a substitute for professional medical advice or medical care. The advice of a medical professional should always be sought prior to commencing any form of medical treatment. To this end, all component information contained within the guidelines is done so for solely educational and scientific purposes. ESTRO and all of its staff, agents and members disclaim any and all warranties and representations with regards to the information contained on the guidelines. This includes any implied warranties and conditions that may be derived from the aforementioned guidelines.

Conflicts of interest:

Ian Paddick works as an ad-hoc consultant for Elekta. All other authors declare no conflicts of interest.

References

[1] Stacchiotti S, Sommer J, Chordoma Global Consensus Group. Building a global consensus approach to chordoma: a position paper from the medical and patient community. Lancet Oncol 2015;16:e71–83.
[2] Aghi MK, Chen CC, Fleseriu M, Newman SA, Lucas JW, Kuo JS, et al. Congress of Neurological Surgeons Systematic Review and Evidence-Based Guidelines on the Management of Patients with Nonfunctioning Pituitary Adenomas: Executive Summary. Neurosurgery 2016;79:521–3.
[3] Goldbrunner R, Minniti G, Preusser M, et al. EANO guidelines for the diagnosis and treatment of meningiomas. Lancet Oncol 2016;17:e383–91.
[4] Sheehan J, Lee CC, Bodach ME, et al. Congress of Neurological Surgeons Systematic Review and Evidence-Based Guideline for the Management of Patients with Residual or Recurrent Nonfunctioning Pituitary Adenomas. Neurosurgery 2016;79:E539–40.
[5] Raverot G, Burman P, McCormack A, et al. European Society of Endocrinology. European Society of Endocrinology Clinical Practice Guidelines for the management of aggressive pituitary tumours and carcinomas. Eur J Endocrinol 2018;178:G1–G24.
[6] Goldbrunner R, Weller M, Regis J, et al. EANO guideline on the diagnosis and treatment of vestibular schwannoma. Neuro Oncol 2020;22:31–45.
[7] Amichetti M, Cianchetti M, Amelio D, Enrici RM, Minniti G. Proton therapy chordoma of the base of the skull: a systematic review. Neurosurg Rev 2009;32:403–16.
[8] Amichetti M, Amelio D, Cianchetti M, Enrici RM, Minniti G. A systematic review of proton therapy in the treatment of chondrosarcoma of the skull base. Neurosurg Rev 2010;33:155–65.
[9] Hankinson TC, Palmeri NO, Williams SA, et al. Patterns of care for craniopharyngioma: survey of members of the American association of neurological surgeons. Pediatr Neurosurg 2013;49:131–6.
[10] Tsao MN, Sahgal A, Xu W, et al. Stereotactic radiosurgery for vestibular schwannoma: International Stereotactic Radiosurgery Society (ISRS) Practice Guideline. J Radiosurg SBRT 2017;5:5–24.
[11] Lee CC, Trifiletti DM, Sahgal A, et al. Stereotactic Radiosurgery for Benign (World Health Organization Grade I) Cavernous Sinus Meningiomas-International Stereotactic Radiosurgery Society (ISRS) Practice Guideline: A Systematic Review. Neurosurgery 2018;83:1128–42.
[12] Kotecha R, Sahgal A, Rubens M, et al. Stereotactic radiosurgery for non-functioning pituitary adenomas: meta-analysis and International Stereotactic Radiosurgery Society practice opinion. Neuro Oncol 2020;22:318–32.
[13] Marchetti M, Sahgal A, De Salles AAF, et al. Stereotactic Radiosurgery for Intracranial Noncavernous Sinus Benign Meningioma: International Stereotactic Radiosurgery Society Systematic Review, Meta-Analysis and Practice Guideline. Neurosurgery 2020. nyaa169.
[14] Combs SE, Farzin M, Boehmer J, et al. Clinical outcome after high-precision radiotherapy for skull base meningiomas: pooled data from three large German centers for radiation oncology. Radiother Oncol 2018;127:274–9.
[15] Amichetti M, Amelio D, Minniti G. Radiosurgery with photons or protons for benign and malignant tumours of the skull base: a review. Radiat Oncol 2012;7:210.
[16] Tseng YD, Hartsell W, Tsai H, et al. Proton therapy patterns of care among pediatric and adult patients with CNS tumors. Neuro Oncol 2018;20:1556–7.
[17] Lesueur P, Calugaru V, Nauraye C, et al. Proton therapy for treatment of intracranial benign tumors in adults: a systematic review. Cancer Treat Rev 2019;72:56–64.
[18] Yamazaki H, Shiomi H, Tsubokura T, et al. Quantitative assessment of inter-observer variability in target volume delineation on stereotactic radiotherapy treatment for pituitary adenoma and meningioma near optic tract. Radiat Oncol 2011;6:10.
[19] Sandström H, Jokura H, Chung C, Toma-Dasu I. Multi-institutional study of the variability in target delineation for six targets commonly treated with radiosurgery. Acta Oncol 2018;57:1515–20.
[20] Growcott S, Dembrey T, Patel R, Eaton D, Cameron A. Inter-observer variability in target volume delineations of benign and metastatic brain tumours for stereotactic radiosurgery: results of a national quality assurance programme. Clin Oncol (R Coll Radiol) 2020;32:13–25.
[21] Seung SK, Larson DA, Galvin JM, et al. American College of Radiology (ACR) and American Society for Radiation Oncology (ASTRO) Practice Guideline for the Performance of Stereotactic Radiosurgery (SRS). Am J Clin Oncol 2013;36:310–5.
[22] Karger CP, Jakel O, Debus J, Kuhn S, Hartmann GH. Three-dimensional accuracy and interfractional reproducibility of patient fixation and positioning using a stereotactic head mask system. Int J Radiat Oncol Biol Phys 2001;49:1493–504.
[23] Khoo VS, Dearnaley DP, et al. Magnetic resonance imaging (MRI): considerations and applications in radiotherapy reatment planning. Radiother Oncol 1997;42:1–15.
[24] Pappas EP, Alshanqity M, Moutsatsos A, et al. MRI-related geometric distortions in stereotactic radiotherapy treatment planning: evaluation and dosimetric impact. Technol Cancer Res Treat 2017;16:1120–9.
[25] Putz F, Mengling V, Perrin R, et al. Magnetic resonance imaging for brain stereotactic radiotherapy: a review of requirements and pitfalls. Strahlenther Onkol 2020;196:444–56.
[26] Fransson A, Andreo P, Pötter R. Aspects of MR image distortions in radiotherapy treatment planning. Strahlenther Onkol 2001;177:59–73.
[27] Fatemi A, Taghizadeh S, Yang CC, Kanakamedala RM, Morris B, Vijayakumar S. Machine-specific magnetic resonance imaging quality control procedures for stereotactic radiosurgery treatment planning. Cureus 2017;9. e1957.
[28] Guckenberger M, Baus WW, Blanck O, et al. Definition and quality requirements for stereotactic radiotherapy: consensus statement from the DEGRO/DGMP Working Group Stereotactic Radiotherapy and Radiosurgery. Strahlenther Onkol 2020;196:417–20.
[29] Hudgins PA, Baugnon KL. Head and neck: skull base imaging. Neurosurgery 2018;82:255–67.
[30] Kelly HR, Curtin HD. Imaging of skull base lesions. Handb Clin Neurol 2016;135:637–57.
[31] Touska P, Connor SEJ. Recent advances in MRI of the head and neck, skull base and cranial nerves: new and evolving sequences, analyses and clinical applications. Br J Radiol 2019;92:20190513.
[32] Wu A, Lindner G, Maitz AH, et al. Physics of gamma knife approach on convergent beams in stereotactic radiosurgery. Int J Radiat Oncol Biol Phys 1990;18:941–9.
[33] Heck B, Jess-Hempen A, Kreiner HJ, Schopgens H, Mack A. Accuracy and stability of positioning in radiosurgery: long-term results of the Gamma Knife system. Med Phys 2007;34:1487–95.
[34] Murphy MJ, Chang SD, Gibbs IC, et al. Patterns of patient movement during frameless image-guided radiosurgery. Int J Radiat Oncol Biol Phys 2003;55:1400–8.
[35] Meyer J, Wilbert J, Baier K, Guckenberger M, Richter A, Sauer O, et al. Positioning accuracy of cone-beam computed tomography in combination with a HexaPOD robot treatment table. Int J Radiat Oncol Biol Phys 2007;67:1220–8.
[36] Ramakrishna N, Rosca F, Friesen S, Tezcanli E, Zygmanszki P, Hacker F. A clinical comparison of patient setup and intra-fraction motion using frame-based radiosurgery versus a frameless image-guided radiosurgery system for intracranial lesions. Radiother Oncol 2010;95:109–15.
[37] Gevaert T, Verellen D, Engels B, et al. Clinical evaluation of a robotic 6-degree of freedom treatment couch for frameless radiosurgery. Int J Radiat Oncol Biol Phys 2012;83:467–74.
[38] Gevaert T, Verellen D, Tournel K, et al. Setup accuracy of the Novalis ExacTrac 6DOF system for frameless radiosurgery. Int J Radiat Oncol Biol Phys 2012;82:1627–35.
[39] Vinod SK, Jameson MG, Min M, Holloway LC. Uncertainties in volume delineation in radiation oncology: a systematic review and recommendations for future studies. Radiother Oncol 2016;121:169–79.
[40] Eekers DB, Int-Ven L, Roelofs E, et al. "European Particle Therapy Network" of ESTRO. The EPTN consensus-based atlas for CT- and MR-based contouring in neuro-oncology. Radiother Oncol 2018;128:37–43.
[41] Chang SD, Main W, Martin DP, Gibbs IC, Heilbrun MP. An analysis of theaccuracy of the CyberKnife: a robotic frameless stereotactic radiosurgical system. Neurosurgery 2003;52:140–6.
[42] Yu C, Jozsef G, Apuzzo ML, Petrovich Z. Dosimetric comparison of CyberKnife with other radiosurgical modalities for an ellipsoidal target. Neurosurgery 2003;53:1155–62.
[43] Kuo JS, Yu C, Petrovich Z, Apuzzo ML. The CyberKnife stereotactic radiosurgery system: description, installation, and an initial evaluation of use and functionality. Neurosurgery 2008;62(Suppl):785–9.
[44] Gevaert T, Levivier M, Lacornerie T, et al. Dosimetric comparison of different treatment modalities for stereotactic radiosurgery of arteriovenous malformations and acoustic neuromas. Radiother Oncol 2013;106:192–7.
[45] Kosaki K, Ecker S, Habermehl D, et al. Comparison of intensity modulated radiotherapy (IMRT) with intensity modulated particle therapy (IMPT) using fixed beams or an ion gantry for the treatment of patients with skull base meningiomas. Radiat Oncol 2012;7:44.
[46] Combs SE, Laperriere N, Brada M. Clinical controversies: proton radiation therapy for brain and skull base tumors. Semin Radiat Oncol 2013;23:120–6.
[47] Combs SE. Does proton therapy have a future in CNS tumors?. Curr Treat Options Neurol 2017;19:12.
[48] Weber DC, Abrunhosa-Branquinho A, Bolsi A, et al. Profile of European proton and carbon ion therapy centers assessed by the EORTC facility questionnaire. Radiother Oncol 2017;124:185–9.
[49] Boehling NS, Grosshans DR, Bluett JB, et al. Dosimetric comparison of three-dimensional conformal proton radiotherapy, intensity-modulated proton therapy, and ntensity-modulated radiotherapy for treatment of pediatric craniopharyngiomas. Int J Radiat Oncol Biol Phys 2012;82:643–52.
[50] Arjomandy SB, Taylor P, Ainsley C, et al. AAPM task group 224: comprehensive proton therapy machine quality assurance. Med Phys 2019;46:e678–705.
[51] Trofimov A, Bortfeld T. Optimization of beam parameters and treatment planning for intensity modulated proton therapy. Technol Cancer Res Treat 2003;2:437–44.
[52] Klimpki G, Psoroulas S, Bula C, et al. A beam monitoring and validation system for continuous line scanning in proton therapy. Phys Med Biol 2017;62:6126–43.
[53] Kanai T, Furuichi W, Mori S. Evaluation of patient positional reproducibility on the treatment couch and its impact on dose distribution using rotating

gantry system in scanned carbon-ion beam therapy. Phys Med 2019;57:160–8.
[54] Lippitz B, Lindquist C, Paddick I, Peterson D, O'Neill K, Beaney R. Stereotactic radiosurgery in the treatment of brain metastases: the current evidence. Cancer Treat Rev 2014;40:48–59.
[55] Paddick I, Lippitz B. A simple dose gradient measurement tool to complement the conformity index. J Neurosurg 2006;105(Suppl):194–201.
[56] Torrens M, Chung C, Chung HT, et al. Standardization of terminology in stereotactic radiosurgery: report from the Standardization Committee of the International Leksell Gamma Knife Society: special topic. J Neurosurg 2014;121(Suppl):2–15.
[57] Emami B, Lyman J, Brown A, et al. Tolerance of normal tissue to therapeutic irradiation. Int J Radiat Oncol Biol Phys 1991;21:109–22.
[58] Tishler RB, Loeffler JS, Lunsford LD, et al. Tolerance of cranial nerves of the cavernous sinus to radiosurgery. Int J Radiat Oncol Biol Phys 1993;27:215–21.
[59] Feigl GC, Bonelli CM, Berghold A, Mokry M. Effects of gamma knife radiosurgery of pituitary adenomas on pituitary function. J Neurosurg 2002;97(5Suppl):415–21.
[60] Timmerman RD. An overview of hypofractionation and introduction to this issue of seminars in radiation oncology. Semin Radiat Oncol 2008;18:215–22.
[61] Bhandare N, Jackson A, Eisbruch A, et al. Radiation therapy and hearing loss. Int J Radiat Oncol Biol Phys 2010;76(3 Suppl):S50–7.
[62] Kirkpatrick JP, van der Kogel AJ, Schultheiss TE. Radiation dose-volume effects in the spinal cord. Int J Radiat Oncol Biol Phys 2010;76(3 Suppl):S42–9.
[63] Lawrence YR, Li XA, el Naqa I, et al. Radiation dose-volume effects in the brain. Int J Radiat Oncol Biol Phys 2010;76(3 Suppl):S20–7.
[64] Leenstra JL, Tanaka S, Kline RW, et al. Factors associated with endocrine deficits after stereotactic radiosurgery of pituitary adenomas. Neurosurgery 2010;67:27–32.
[65] Mayo C, Yorke E, Merchant TE. Radiation associated brainstem injury. Int J Radiat Oncol Biol Phys 2010;76(3 Suppl):S36–41.
[66] Mayo C, Martel MK, Marks LB, Flickinger J, Nam J, Kirkpatrick J. Radiation dose-volume effects of optic nerves and chiasm. Int J Radiat Oncol Biol Phys 2010;76(3 Suppl):S28–35.
[67] Marek J, Jezková J, Hána V, Krsek M, et al. Is it possible to avoid hypopituitarism after irradiation of pituitary adenomas by the Leksell gamma knife?. Eur J Endocrinol 2011;164:169–78.
[68] Sheehan JP, Pouratian N, Steiner L, Laws ER, Vance ML. Gamma Knife surgery for pituitary adenomas: factors related to radiological and endocrine outcomes. J Neurosurg 2011;114:303–9.
[69] Leavitt JA, Stafford SL, Link MJ, Pollock BE. Long-term evaluation of radiation-induced optic neuropathy after single-fraction stereotactic radiosurgery. Int J Radiat Oncol Biol Phys 2013;87:524–7.
[70] Sicignano G, Losa M, del Vecchio A, et al. Dosimetric factors associated with pituitary function after Gamma Knife Surgery (GKS) of pituitary adenomas. Radiother Oncol 2012;104:119–24.
[71] Gondi V, Hermann BP, Mehta MP, Tomé WA. Hippocampal dosimetry predicts neurocognitive function impairment after fractionated stereotactic radiotherapy for benign or low-grade adult brain tumors. Int J Radiat Oncol Biol Phys 2013;85:348–54.
[72] Minniti G, Scaringi C, Paolini S, et al. Single-fraction versus multifraction (3 x 9 Gy) stereotactic radiosurgery for large (>2 cm) brain metastases: a comparative analysis of local control and risk of radiation-induced brain necrosis. Int J Radiat Oncol Biol Phys 2016;95:1142–8.
[73] Niyazi M, Niemierko A, Paganetti H, et al. Volumetric and actuarial analysis of brain necrosis in proton therapy using a novel mixture cure model. Radiother Oncol 2020;142:154–61.
[74] Lambrecht M, Eekers DBP, Alapetite C, et al. work package 1 of the taskforce "European Particle Therapy Network" of ESTRO. Radiation dose constraints for organs at risk in neuro-oncology; the European Particle Therapy Network consensus. Radiother Oncol 2018;128:26–36.
[75] Ferrante L, Trillò G, Ramundo E, et al. Surgical treatment of pituitary tumors in the elderly: clinical outcome and long-term follow-up. J Neurooncol 2002;60:185–91.
[76] Murad MH, Fernández-Balsells MM, Barwise A, et al. Outcomes of surgical treatment for nonfunctioning pituitary adenomas: a systematic review and meta-analysis. Clin Endocrinol (Oxf) 2003;73:777–91.
[77] Mortini P, Losa M, Barzaghi R, Boari N, Giovanelli M. Results of transsphenoidal surgery in a large series of patients with pituitary adenoma. Neurosurgery 2005;56:1222–33.
[78] Cappabianca P, Cavallo LM, Solari D, Esposito F. Endoscopic endonasal transsphenoidal approach to pituitary adenomas. J Neurosurg 2015;122:473–4.
[79] Minniti G, Osti MF, Niyazi M. Target delineation and optimal radiosurgical dose for pituitary tumors. Radiat Oncol 2016;11:135.
[80] Iwata H, Sato K, Tatewaki K, et al. Hypofractionated stereotactic radiotherapy with CyberKnife for nonfunctioning pituitary adenoma: high local control with low toxicity. Neuro Oncol 2011;13:916–22.
[81] Minniti G, Scaringi C, Poggi M, et al. Fractionated stereotactic radiotherapy for large and invasive non-functioning pituitary adenomas: long-term clinical outcomes and volumetric MRI assessment of tumor response. Eur J Endocrinol 2015;172:433–41.
[82] Louis DN, Perry A, Reifenberger G, et al. The 2016 World Health Organization Classification of Tumors of the Central Nervous System: a summary. Acta Neuropathol 2016;131:803–20.
[83] Brastianos PK, Galanis E, Butowski N, et al. International Consortium on Meningiomas. Advances in multidisciplinary therapy for meningiomas. Neuro Oncol 2019;21(Suppl 1):i18–31.
[84] Minniti G, Amichetti M, Enrici RM. Radiotherapy and radiosurgery for benign skull base meningiomas. Radiat Oncol 2009;4:42.
[85] Combs SE, Adeberg S, Dittmar JO, et al. Skull base meningiomas: long-term results and patient self-reported outcome in 507 patients treated with fractionated stereotactic radiotherapy (FSRT) or intensity modulated radiotherapy (IMRT). Radiother Oncol 2013;106:186–91.
[86] Pinzi V, Biagioli E, Roberto A, et al. Radiosurgery for intracranial meningiomas: a systematic review and meta-analysis. Crit Rev Oncol Hematol 2017;113:122–34.
[87] Murray FR, Snider JW, Bolsi A, et al. Long-term clinical outcomes of pencil beam scanning proton therapy for benign and non-benign intracranial meningiomas. Int J Radiat Oncol Biol Phys 2017;99:1190–8.
[88] Sanford NN, Yeap BY, Larvie M, et al. Prospective, randomized study of radiation dose escalation with combined proton-photon therapy for benign meningiomas. Int J Radiat Oncol Biol Phys 2017;99:787–96.
[89] Rogers L, Zhang P, Vogelbaum MA, et al. Intermediate-risk meningioma: initial outcomes from NRG Oncology RTOG 0539. J Neurosurg 2018;129:35–47.
[90] Rogers CL, Won M, Vogelbaum MA, et al. High-risk meningioma: initial outcomes from NRG oncology/RTOG 0539. Int J Radiat Oncol Biol Phys 2020;106:790–9.
[91] Weber DC, Ares C, Villa S, et al. Adjuvant postoperative high-dose radiotherapy for atypical and malignant meningioma: a phase-II parallel non-randomized and observation study (EORTC 22042–26042). Radiother Oncol 2018;128:260–5.
[92] Jenkinson MD, Javadpour M, Haylock BJ, et al. The ROAM/EORTC-1308 trial: radiation versus observation following surgical resection of atypical meningioma: study protocol for a randomised controlled trial. Trials 2015;16:519.
[93] Watts J, Box G, Galvin A, Brotchie P, Trost N, Sutherland T. Magnetic resonance imaging of meningiomas: a pictorial review. Insights Imaging 2014;5:113–22.
[94] Huang RY, Bi WL, Griffith B, et al. International Consortium on Meningiomas. Imaging and diagnostic advances for intracranial meningiomas. Neuro Oncol 2019;21:i44–61.
[95] Rutten I, Cabay JE, Withofs N, Lemaire C, Aerts J, Baart V, et al. PET/CT of skull base meningiomas using 2–18F-fluoro-L-tyrosine: initial report. J Nucl Med 2007;48:720–5.
[96] Astner ST, Dobrei-Ciuchendea M, Essler M, Bundschuh RA, Sai H, Schwaiger M, et al. Effect of 11C-methionine-positron emission tomography on gross tumor volume delineation in stereotactic radiotherapy of skull base meningiomas. Int J Radiat Oncol Biol Phys 2008;72:1161–7.
[97] Gehler B, Paulsen F, Oksüz MO, Hauser TK, Eschmann SM, Bares R, et al. [68Ga]-DOTATOC-PET/CT for meningioma IMRT treatment planning. Radiat Oncol 2009;4:56.
[98] Grosu AL, Weber WA. PET for radiation treatment planning of brain tumours. Radiother Oncol 2010;96:325–7.
[99] Combs SE, Welzel T, Habermehl D, et al. Prospective evaluation of early treatment outcome in patients with meningiomas treated with particle therapy based on target volume definition with MRI and 68Ga-DOTATOC-PET. Acta Oncol 2013;52:514–20.
[100] Afshar-Oromieh A, Wolf MB, et al. Comparison of (6)(8)Ga-DOTATOC-PET/CT and PET/MRI hybrid systems in patients with cranial meningioma: Initial results. Neuro Oncol 2015;17:312–9.
[101] Dittmar JO, Kratochwil C, Dittmar A, et al. First intraindividual comparison of contrast-enhanced MRI, FET- and DOTATOC- PET in patients with intracranial meningiomas. Radiat Oncol 2017;12:169.
[102] Kessel KA, Weber W, Yakushev I, et al. Integration of PET-imaging into radiotherapy treatment planning for low-grade meningiomas improves outcome. Eur J Nucl Med Mol Imaging 2020;47:1391–9.
[103] Nägele T, Petersen D, Klose U, Grodd W, Opitz H, Voigt K. The, "dural tail" adjacent to meningiomas studied by dynamic contrast-enhanced MRI: a comparison with histopathology. Neuroradiology 1994;36:303–7.
[104] Kawahara Y, Niiro M, Yokoyama S, Kuratsu J. Dural congestion accompanying meningioma invasion into vessels: the dural tail sign. Neuroradiology 2001;43:462–5.
[105] Perry A, Gutmann DH, Reifenberger G. Molecular pathogenesis of meningiomas. J Neurooncol 2004;70:183–202.
[106] Sotoudeh H, Yazdi HR. A review on dural tail sign. World J Radiol 2010;2:188–92.
[107] Kondziolka D, Flickinger JC, Perez B. Judicious resection and/or radiosurgery for parasagittal meningiomas: outcomes from a multicenter review. Gamma Knife Meningioma Study Group. Neurosurgery 1998;43:405–13.
[108] DiBiase SJ, Kwok Y, Yovino S, et al. Factors predicting local tumor control after gamma knife stereotactic radiosurgery for benign intracranial meningiomas. Int J Radiat Oncol Biol Phys 2004;60:1515–9.
[109] Rogers L, Jensen R, Perry A. Chasing your dural tail: factors predicting local tumor control after gamma knife stereotactic radiosurgery for benign intracranial meningiomas: In regard to DiBiase et al. (Int J Radiat Oncol Biol Phys 2004;60:1515-1519). Int J Radiat Oncol Biol Phys 2005;62:616–8.
[110] Mortini P, Losa M, Pozzobon G, et al. Neurosurgical treatment of craniopharyngioma in adults and children: early and long-term results in a large case series. J Neurosurg 2011;114:1350–9.

[111] Buchfelder M, Schlaffer SM, Lin F, Kleindienst A. Surgery for craniopharyngioma. Pituitary 2013;16:18–25.
[112] Lo AC, Howard AF, Nichol A, et al. Long-term outcomes and complications in patients with craniopharyngioma: the British Columbia Cancer Agency experience. Int J Radiat Oncol Biol Phys 2014;88:1011–8.
[113] Varlotto J, DiMaio C, Grassberger C, et al. Multi-modality management of craniopharyngioma: a review of various treatments and their outcomes. Neurooncol Pract 2016;3:173–87.
[114] Lin Y, Hansen D, Sayama CM, Pan IW, Lam S. Transfrontal and transsphenoidal approaches to pediatric craniopharyngioma: a national perspective. Pediatr Neurosurg 2017;52(3):155–60.
[115] Rajan B, Ashley S, Gorman C, et al. Craniopharyngioma–a long-term results following limited surgery and radiotherapy. Radiother Oncol 1993;26:1–10.
[116] Scott RM, Hetelekidis S, Barnes PD, Goumnerova L, Tarbell NJ. Surgery, radiation, and combination therapy in the treatment of childhood craniopharyngioma–a 20-year experience. Pediatr Neurosurg 1994;21(Suppl 1):75–81.
[117] Stripp DC, Maity A, Janss AJ, et al. Surgery with or without radiation therapy in the management of craniopharyngiomas in children and young adults. Int J Radiat Oncol Biol Phys 2004;58:714–20.
[118] Schoenfeld A, Pekmezci M, Barnes MJ, et al. The superiority of conservative resection and adjuvant radiation for craniopharyngiomas. J Neurooncol 2012;108:133–9.
[119] Masson-Cote L, Masucci GL, Atenafu EG, et al. Long-term outcomes for adult craniopharyngioma following radiation therapy. Acta Oncol 2013;52:153–8.
[120] Minniti G, Saran F, Traish D, et al. Fractionated stereotactic conformal radiotherapy following conservative surgery in the control of craniopharyngiomas. Radiother Oncol 2007;82:90–5.
[121] Beltran C, Roca M, Merchant TE. On the benefits and risks of proton therapy in pediatric craniopharyngioma. Int J Radiat Oncol Biol Phys 2012;82:e281–7.
[122] Harrabi SB, Adeberg S, Welzel T, et al. Long term results after fractionated stereotactic radiotherapy (FSRT) in patients with craniopharyngioma: maximal tumor control with minimal side effects. Radiat Oncol 2014;9:203.
[123] Albano L, Losa M, Flickinger JC, Mortini P, Minniti G. Radiotherapy of parasellar tumours. Neuroendocrinology 2020.
[124] Kobayashi T, Kida Y, Mori Y, et al. Long-term results of gamma knife surgery for the treatment of craniopharyngioma in 98 consecutive cases. J Neurosurg 2005;103:482–8.
[125] Lee M, Kalani MY, Cheshier S, et al. Radiation therapy and CyberKnife radiosurgery in the management of craniopharyngiomas. Neurosurg Focus 2008;24:E4.
[126] Niranjan A, Kano H, Mathieu D, et al. Radiosurgery for craniopharyngioma. Int J Radiat Oncol Biol Phys 2010;78:64–71.
[127] Iwata H, Tatewaki K, Inoue M, et al. Single and hypofractionated stereotactic radiotherapy with CyberKnife for craniopharyngioma. J Neurooncol 2012;106:571–7.
[128] Saleem MA, Hashim AS, Rashid A, Ali M. Role of gamma knife radiosurgery in multimodality management of craniopharyngioma. Acta Neurochir Suppl 2013;116:55–60.
[129] Lee CC, Yang HC, Chen CJ, et al. Gamma Knife surgery for craniopharyngioma: report on a 20-year experience. J Neurosurg 2014;121(Suppl):167–78.
[130] Lamiman K, Wong KK, Tamrazi B, et al. A quantitative analysis of craniopharyngioma cyst expansion during and after radiation therapy and surgical implications. Neurosurg Focus 2016;41(6):E15.
[131] Shirato H, Sakamoto T, Sawamura Y, et al. Comparison between observation policy and fractionated stereotactic radiotherapy (SRT) as an initial management for vestibular schwannoma. Int J Radiat Oncol Biol Phys 1999;44:545–50.
[132] Charabi S, Tos M, Thomsen J, Charabi B, Mantoni M. Vestibular schwannoma growth: the continuing controversy. Laryngoscope 2000;110:1720–5.
[133] Agrawal Y, Clark JH, Limb CJ, Niparko JK, Francis HW. Predictors of vestibular schwannoma growth and clinical implications. Otol Neurotol 2010;31:807–12.
[134] Irving RM, Harada T, Moffat DA, et al. Somatic neurofibromatosis type 2 gene mutations and growth characteristics in vestibular schwannoma. Am J Otol 1997;18:754–60.
[135] Nguyen T, Chung LK, Sheppard JP, et al. Surgery versus stereotactic radiosurgery for the treatment of multiple meningiomas in neurofibromatosis type 2: illustrative case and systematic review. Neurosurg Rev 2019;42:85–96.
[136] Kirchmann M, Karnov K, Hansen S, Dethloff T, Stangerup SE, Caye-Thomasen P. Ten-year follow-up on tumor growth and hearing in patients observed with an intracanalicular vestibular schwannoma. Neurosurgery 2017;80(1):49–56.
[137] Tonn JC, Schlake HP, Goldbrunner R, Milewski C, Helms J, Roosen K. Acoustic neuroma surgery as an interdisciplinary approach: a neurosurgical series of 508 patients. J Neurol Neurosurg Psychiatry 2000;69:161–6.
[138] Samii M, Metwali H, Gerganov V. Efficacy of microsurgical tumor removal for treatment of patients with intracanalicular vestibular schwannoma presenting with disabling vestibular symptoms. J Neurosurg 2017;126:1514–9.
[139] Gardner G, Robertson JH. Hearing preservation in unilateral acoustic neuroma surgery. Ann Otol Rhinol Laryngol 1988;97:55–66.
[140] Carlson ML, Vivas EX, McCracken DJ, et al. Congress of neurological surgeons systematic review and evidence-based guidelines on hearing preservation outcomes in patients with sporadic vestibular schwannomas. Neurosurgery 2018;82:E35–9.
[141] Morton RP, Ackerman PD, Pisansky MT, et al. Prognostic factors for the incidence and recovery of delayed facial nerve palsy after vestibular schwannoma resection. J Neurosurg 2011;114:375–80.
[142] Samii M, Metwali H, Gerganov V. Microsurgical management of vestibular schwannoma after failed previous surgery. J Neurosurg 2016;125:1198–203.
[143] Combs SE, Thilmann C, Debus J, Schulz-Ertner D. Long-term outcome of stereotactic radiosurgery (SRS) in patients with acoustic neuromas. Int J Radiat Oncol Biol Phys 2006;64(5):1341–7.
[144] Myrseth E, Møller P, Pedersen PH, Lund-Johansen M. Vestibular schwannoma: surgery or gamma knife radiosurgery? A prospective, nonrandomized study. Neurosurgery 2009;64:654–61.
[145] Combs SE, Welzel T, Schulz-Ertner D, Huber PE, Debus J. Differences in clinical results after LINAC-based single-dose radiosurgery versus fractionated stereotactic radiotherapy for patients with vestibular schwannomas. Int J Radiat Oncol Biol Phys 2010;76:193–200.
[146] Flickinger JC, Kondziolka D, Niranjan A, Lunsford LD. Results of acoustic neuroma radiosurgery: an analysis of 5 years' experience using current methods. J Neurosurg 2013;119(Suppl):1–6.
[147] Lunsford LD, Niranjan A, Flickinger JC, Maitz A, Kondziolka D. Radiosurgery of vestibular schwannomas: summary of experience in 829 cases. J Neurosurg 2013;119(Suppl):195–9.
[148] Régis J, Carron R, Delsanti C, Porcheron D, et al. Radiosurgery for vestibular schwannomas. Neurosurg Clin N Am 2013;24:521–30.
[149] Kim H, Potrebko P, Rivera A, et al. Tumor volume threshold for achieving improved conformity in VMAT and Gamma Knife stereotactic radiosurgery for vestibular schwannoma. Radiother Oncol 2015;115:229–34.
[150] Golfinos JG, Hill TC, Rokosh R, et al. A matched cohort comparison of clinical outcomes following microsurgical resection or stereotactic radiosurgery for patients with small- and medium-sized vestibular schwannomas. J Neurosurg 2016;125:1472–82.
[151] Berkowitz O, Han YY, Talbott EO, et al. Gamma knife radiosurgery for vestibular schwannomas and quality of life evaluation. Stereotact Funct Neurosurg 2017;95:166–73.
[152] Collen C, Ampe B, Gevaert T, et al. Single fraction versus fractionated linac-based stereotactic radiotherapy for vestibular schwannoma: a single-institution experience. Int J Radiat Oncol Biol Phys 2011;81:e503–9.
[153] Combs SE, Welzel T, Kessel K, et al. Hearing preservation after radiotherapy for vestibular schwannomas is comparable to hearing deterioration in healthy adults and is accompanied by local tumor control and a highly preserved quality of life (QOL) as patients' self-reported outcome. Radiother Oncol 2013;106:175–80.
[154] Combs SE, Engelhard C, Kopp C, et al. Long-term outcome after highly advanced single-dose or fractionated radiotherapy in patients with vestibular schwannomas - pooled results from 3 large German centers. Radiother Oncol 2015;114:378–83.
[155] Germano IM, Sheehan J, Parish J, et al. Congress of neurological surgeons systematic review and evidence-based guidelines on the role of radiosurgery and radiation therapy in the management of patients with vestibular schwannomas. Neurosurgery 2018;82:E49–51.
[156] Hansasuta A, Choi CY, Gibbs IC, et al. Multisession stereotactic radiosurgery for vestibular schwannomas: single-institution experience with 383 cases. Neurosurgery 2011;69:1200–9.
[157] Nguyen T, Duong C, Sheppard JP, et al. Hypo-fractionated stereotactic radiotherapy of five fractions with linear accelerator for vestibular schwannomas: a systematic review and meta-analysis. Clin Neurol Neurosurg 2018;166:116–23.
[158] Di Maio S, Rostomily R, Sekhar LN. Current surgical outcomes for cranial bas chordomas. Cohort study of 95 patients. Neurosurgery 2012;70:1355–60.
[159] Ouyang T, Zhang N, Zhang Y, et al. Clinical characteristics, immunohistochemistry, and outcomes of 77 patients with skull base chordomas. World Neurosurg 2014;81:790–7.
[160] Wang L, Wu Z, Tian K, et al. Clinical features and surgical outcomes of patients with skull base chordoma: a retrospective analysis of 238 patients. J Neurosurg 2017;127:1257–67.
[161] McDonald MW, Linton OR, Moore MG, Ting JY, Cohen-Gadol AA, Shah MV. Influence of residual tumor volume and radiation dose coverage in outcomes for clival chordoma. Int J Radiat Oncol Biol Phys 2016;95:304–11.
[162] Weber DC, Malyapa R, Albertini F, et al. Long term outcomes of patients with skull- base low-grade chondrosarcoma and chordoma patients treated with pencil beam scanning proton therapy. Radiother Oncol 2016;120:169–74.
[163] Fung V, Calugaru V, Bolle S, et al. Proton beam therapy for skull base chordomas in 106 patients: A dose adaptive radiation protocol. Radiother Oncol 2018;128:198–202.
[164] Stacchiotti S, Gronchi A, Fossati P, et al. Best practices for the management of local-regional recurrent chordoma: a position paper by the Chordoma Global Consensus Group. Ann Oncol 2017;28:1230–42.
[165] Debus J, Schulz-Ertner D, Schad L, et al. Stereotactic fractionated radiotherapy for chordomas and chondrosarcomas of the skull base. Int J Radiat Oncol Biol Phys 2000;47:591–6.
[166] Dassoulas K, Schlesinger D, Yen CP, Sheehan J. The role of Gamma Knife surgery in the treatment of skull base chordomas. J Neurooncol 2009;94:243–8.

[167] Bugoci DM, Girvigian MR, Chen JC, Miller MM, Rahimian J. Photon-based fractionated stereotactic radiotherapy for postoperative treatment of skull base chordomas. Am J Clin Oncol 2013;36:404–10.
[168] Sahgal A, Chan MW, Atenafu EG, Masson-Cote L, Bahl G, Yu E, et al. Image-guided, intensity-modulated radiation therapy (IG-IMRT) for skull base chordoma and chondrosarcoma: preliminary outcomes. Neuro Oncol 2015;17:889–94.
[169] Kano H, Sheehan J, Sneed PK, et al. Skull base chondrosarcoma radiosurgery: report of the North American Gamma Knife Consortium. J Neurosurg 2015;123:1268–75.
[170] Zhou J, Yang B, Wang X, Jing Z. Comparison of the effectiveness of radiotherapy with photons and particles for chordoma after surgery: a meta-analysis. World Neurosurg 2018;117:46–53.
[171] Weber DC, Badiyan S, Malyapa R, et al. Long-term outcomes and prognostic factors of skull-base chondrosarcoma patients treated with pencil-beam scanning proton therapy at the Paul Scherrer Institute. Neuro-oncology 2016;18:236–324.
[172] Vogin G, Calugaru V, Bolle S, et al. Investigation of ectopic recurrent skull base and cervical chordomas: The Institut Curie's proton therapy center experience. Head Neck 2016;38(Suppl 1):E1238–46.